OPEN ACCESS Freely available online

ISSN 2737-5323
Volume 5, Issue 1
https://afm.iikii.com.sg/
Applied Functional Materials

Article

Numerical Simulation of Aerodynamics Effect by Surface Modification in S1210 and S1223 Airfoils Under Martian Conditions

Wen-Chung Wu [1,]*, Saswata Daw [1] and Durgawati Sharma [2]

[1] Department of Aeronautical Engineering, National Formosa University, Huwei, 632, Taiwan; saswatadaw@gmail.com
[2] Department of BioTechnology Engineering, National Formosa University, Huwei, 632, Taiwan; watisharma1810@gmail.com
* Correspondence: wuwenj@nfu.edu.tw

Received: Nov 28, 2024; **Revised:** Dec 20, 2024; **Accepted:** Dec 22, 2024; **Published:** Mar 13, 2025

Abstract: The performance analysis of airfoils in the extraterrestrial atmosphere is important in the design of drones and aircraft operating in Martian conditions. In this study, we numerically simulated the aerodynamic behavior of modified S1210 and S1223 airfoils. Their geometric surfaces such as dimples and protrusions were modified to improve their aerodynamic characteristics. The airfoil with a chord length of 1 m was modified and implemented on the upper surface of a 2-dimensional airfoil model and placed at the position of 70% of the chord length. Computational fluid dynamics (CFD) was used to evaluate the aerodynamic performance of the S1223 and S1210 airfoils. The Airfoils were tested at different angles of attack (AOA) to figure out the lift and drag coefficients, and the Cl/Cd ratio was determined in the aerodynamic performance of different flight scenarios. Reynolds numbers 20000–40000 and the AOA between -4 to 20° for S1210 and S1223 airfoils were considered. The S1210 and S1223 airfoils showed delayed stall traits. The modifications increased the stall trait and improved the Cl/Cd performance, especially for the semicircular and V-shaped inward and outward bulges. For five different modifications of the S1210 airfoils with a normal outward bulge, V-shaped inward and outward bulges, and semicircular inward and outward bulges were observed. The geometry of the normal outward bulge did not show much promising result compared with that of the S1210 airfoil without modification. The protrusion on the surface of the airfoil benefited the aerodynamic performance of the airfoil in Martian conditions.

Keywords: Modified S1210 and S1223 airfoil, Computational fluid dynamics, Aerodynamic performance, Surface modification of airfoil

1. Introduction

The aerodynamic performance of airfoils under extraterrestrial conditions, particularly in the Martian atmosphere, has gained increasing interest due to ongoing space exploration missions and future Mars colonization. One of the primary challenges in Martian aerodynamics is the design and optimization of airfoils for efficient flight in low-Reynolds number (Re) environments. Mars' atmosphere has approximately a 1% density of Earth's and presents unique challenges for aerodynamic performance, necessitating precise modifications to airfoil geometry to enhance lift and minimize drag. A previous study [1] showed that surface modifications, such as dimples, induced turbulence, delayed boundary layer separation, and decreased wake formation and pressure drag. Aircraft on Mars need to fly at much lower speeds and use larger wing areas than on Earth to achieve the same level of lift [2]. The low atmospheric density needs the airfoils of Mars aircraft to especially operate in compressible, low Re flow.

Therefore, it is essential to improve lift and increase the angle of attack (AOA) at which stall occurs. Selig *et al.* demonstrated that the S1210 airfoil exhibits favorable characteristics in terms of delayed boundary layer separation and reduced drag at low-Re for extraterrestrial applications such as Martian exploration [3]. The result of numerical optimization of Mars Airplane’s airfoil at Re = 105 and M = 0.47 also indicates that thin airfoils enable good performance at low Re. At low Re, complicated flow phenomena including separation, transition, and reattachment take place on the wing surface which strongly affects its flight performance. Particularly, laminar separation bubbles play an important role in determining pressure distributions on the wing and aerodynamic characteristics [4]. The S1223 airfoil is particularly well-suited for Martian conditions due to its superior performance in low-Re environments, which are typical in the thin Martian atmosphere. Its design provides high lift-to-drag ratios, which is essential for efficient flight in Mars' atmosphere, where the air density is only about 1% of Earth's. The S1223 airfoil shows its ability to generate substantial lift while minimizing drag, making it ideal for applications where maximizing aerodynamic efficiency in a low-density environment is critical.

Based on the previous results, we investigated the effect of geometric protrusions on the aerodynamic performance of S1210 and S1223 airfoils at low Re. For low-speed incompressible flows, the physics of flow separation is heavily influenced by viscous effects, forming large-scale vortices. Munday *et al.* explored airfoil performance at Re of between 3,000 and 10,000 [5]. The protrusions were introduced at the trailing edge of the airfoil, and five different types of protrusions were tested for each airfoil. The resulting aerodynamic performance enhancements were analyzed and compared with those of normal airfoils. There was a significant enhancement observed for the S1210 and S1223 airfoils. Their performance was better than normal airfoils. The S1210 airfoil's performance was better than the S1223 airfoils. AOA ranged between -4 to 20 °.

Commented [U1]: No reference for this. Please add it.

Commented [SD2R1]: Updated

2. Airfoil Design

Four types of airfoil protrusions were experimented with in this study: V-shaped inward and outward bulges, and semicircular inward and outward bulges. The modified airfoils were S1210 and S1223. The modification was made at the trailing edge of the airfoil at a distance of 0.7m of the total chord length. The modification was designed using the ANSYS design modular.

3. Methodology and Governing Equation

The Navier-Stokes equation governs flow over an aerofoil, ignoring the source terms the governing equations can be noted down as below:

$$\frac{\partial\rho}{\partial t}+\frac{\partial(\rho u)}{\partial x}+\frac{\partial(\rho v)}{\partial y}=0 \tag{1}$$

$$\rho(u\frac{\partial u}{\partial x}+v\frac{\partial u}{\partial y}) = -\frac{\partial P}{\partial x}+y_x+\frac{\partial}{\partial x}\left(\frac{-2}{3}\mu\left(\frac{\partial v}{\partial y}\right)+2\mu\frac{\partial u}{\partial x}\right)+\frac{\partial}{\partial y}(\mu)[\frac{\partial v}{\partial x}+\frac{\partial u}{\partial y}] \tag{2}$$

$$\rho(u\frac{\partial u}{\partial x}+v\frac{\partial u}{\partial y}) = -\frac{\partial P}{\partial x}+y_y+\frac{\partial}{\partial y}\left(\frac{-2}{3}\mu\left(\frac{\partial v}{\partial y}\right)+2\mu\frac{\partial u}{\partial y}\right)+\frac{\partial}{\partial x}(\mu)[\frac{\partial v}{\partial x}+\frac{\partial u}{\partial y}] \tag{3}$$

Steady flow conditions, constant density (ρ), and constant fluid viscosity (μ) were assumed in this study. Since the flow over the airfoil is governed by the Navier-Stokes equations, by neglecting source terms, the simplified governing equations for the flow were established. In these equations, v represents the kinematic viscosity, u is the fluid velocity, p is the pressure, ρ is the fluid density, and μ is the dynamic viscosity.

Computational fluid dynamics (CFD) were used in simulations using ANSYS Fluent, a widely-used CFD software. The Martian atmosphere was modelled with a pressure of 610 *P*a and carbon dioxide (CO_2). The airfoils were analysed at the Re of 20,000 and 40,000, which correspond to typical operational conditions for Martian flight.

In this study, a pressure-based solver was utilized, and the Spalart-Allmaras turbulence model, a one-equation model, was employed to simulate the turbulence effects. Simulations were performed for angles of attack ranging from -4° to 20° with 2° increments. For the low Re inlet condition, the boundary conditions of velocity inlet in the pressure far-field conditions were assumed. A no-slip boundary condition was imposed on the airfoil surface, and wall boundary conditions were applied at the top and bottom computational domain boundaries. The residual taken into consideration was 10^{-5}. The atmospheric conditions used in the numerical analysis are presented in Table 1.

Table 1. Parameters in simulation of modified airfoils.

Parameters	Mars Atmosphere
Gravitational Acceleration	3.71m/s^2
Prandtl Number	0.7
Density	0.015 kg/m^3
Viscosity	1.13e-05
Velocity	15.0666 m/s (Re = 20,000)
Pressure	703 Pa

The chord length of each airfoil in this numerical analysis was 1 m. Geometry was created by the ANSYS design module. For the boundary around the airfoil, a simple rectangle geometry was used. The dimensions used for the 2D analysis was H4 =10*c* (*c*=chord lenth of aerofoil), H5 = 25*c*, V6 = 10*c*, and V7 =10*c*.The airfoils were surrounded by a structured mesh, with a fine grid near the surface to accurately capture boundary layer effects. To ensure critical flow features were resolved accurately, 100,000 cells were utilized for 2D geometry.

4. Results

The results were compared with those of normal S1210 and S1223 to check which airfoil performance in the Martian conditions.

4.1. Cl/Cd of Normal S1210 and S1223 Airfoil at Re 20,000 and 40,000

Figure 1 illustrates the aerodynamic performance of both airfoils at a low Re of 20,000. The Cl/Cd ratio for both airfoils increased as the AOA rose from -4° to 6°. Beyond this point, the ratio gradually decreased with increasing angles, indicating a drop in aerodynamic efficiency. The S1210 airfoil (the blue line) achieved its peak Cl/Cd ratio of approximately 25 at an AOA between 6° and 8°, indicating optimal performance, where high lift was generated with minimal drag. In comparison, the S1223 airfoil (in orange line) reached its maximum Cl/Cd ratio of around 20 at an AOA between 4° and 6°, slightly lower than the S1210. At angles exceeding 10°, both airfoils experienced a significant decline in their Cl/Cd ratios. However, the S1210 maintained marginally better performance at higher angles. At negative angles of attack (-4° to 0°), the S1223 airfoil outperformed the S1210, displaying a positive Cl/Cd, whereas the S1210 struggled with negative or low values in the range. Overall, the S1210 airfoil demonstrated a higher lift-to-drag ratio across a broader range of AOA, making it more aerodynamically efficient, particularly in the moderate angle range. On the other hand, the S1223 airfoil showed superior performance at negative and lower angles of attack, though it did not show the same peak efficiency as the S1210.

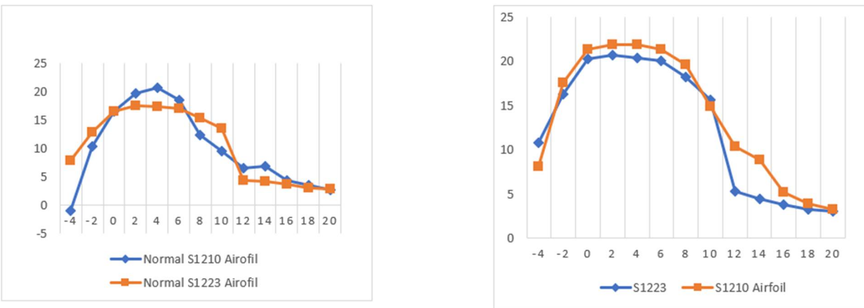

(a) Cl/Cd of Re 20000 (b) Cl/Cd of Re 40000

Fig. 1. Cl/Cd at Re 20,000 and 40,000.

Commented [AZ3]: Please note that all figures in the main text need to be non-editable images.

At a Re of 40,000, the S1210 airfoil consistently showed a higher Cl/Cd ratio than the S1223 airfoil across most angles of attack. While the S1223 airfoil performed similarly at lower angles, its efficiency decreased rapidly beyond 10°. The S1210 airfoil showed its peak Cl/Cd ratio between 6° and 8° with a maximum of higher than 21. In contrast, the S1223 airfoil showed a peak earlier between 4° and 6°, with a maximum Cl/Cd of 20. Overall, the S1210 airfoil maintained slightly better aerodynamic efficiency, holding its peak performance for a longer range of angles. After hitting their peak, both airfoils showed worsened performance. The S1223 airfoil's performance decreased beyond 10° with the Cl/Cd lower than 5 by 14° and negligible by 18° to 20°. Meanwhile, the S1210 airfoil maintained its Cl/Cd higher than the S1223 airfoil up to around 14°, though it declined by 20°. Even at a Re of 40,000, the S1210 airfoil outperformed the S1223 in terms of Cl/Cd and overall efficiency, especially in the moderate positive angle range of 4° to 10°. Both airfoils experienced stall at higher angles, but the S1210 handled it gradually as a more reliable option when the airfoil operated beyond its optimal AOA.

4.2. Cl/Cd of *Modified S1210 and S1223* A*irfoil at* Re *20,000 and 40,000*

The Cl/Cd ratio was analysed to explore how the geometric modification enhanced the performance of the airfoil and how the stall angle increased due to the early boundary layer separation and the intrusion in the surface of the airfoil. At 20,000 Re, the S1210 airfoil increased its performance which was significantly worsened after a peak. It performed worse than the modified airfoil with negative values at higher AOAs. The modified airfoils performed better than the normal airfoils in the AOA of -4 to 16°. The curves for the semi-circular inward bulge (the orange line), semi-circular outward bulge (the grey line), and V-shaped bulge inward (the yellow line) were closely aligned which showed similar performance (Fig. 2). The V-shaped bulge outward (the light blue line) presented similar performance around 12°, but then it performed worse than the other modified airfoils. The modifications to the S1210 airfoil improved performance significantly compared with the normal airfoil. At Re 40,000, the S1210 airfoil consistently performed worse than the modified airfoils, especially between the AOA of 8 to 16°. Similar to Fig. 1(a), all modified airfoils performed better than the normal airfoils. All modified airfoils had higher peak values (25–30) than the normal airfoil, maintaining superior performance in the AOA between 4 and 14°. At a Re of 40,000, the modified S1210 airfoil showed superior performance across a wide range of Re than the normal version.

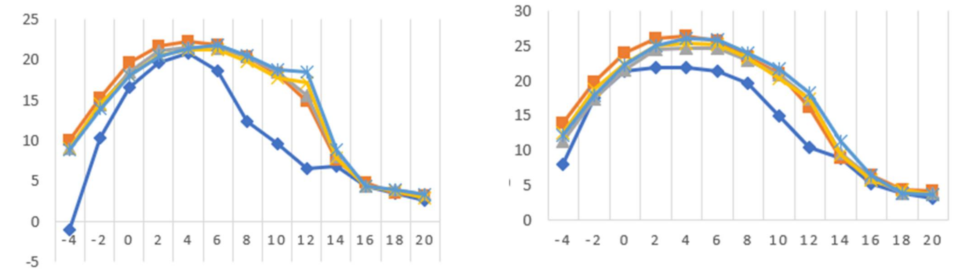

(a) Re 20000 (b) Re 40000

Fig. 2. Cl/Cd of modified S1210 at Re 20,000 and 40,000.

Commented [AZ4]: Please note that all figures in the main text need to be non-editable images.

4.3. Cl/Cd Performance at 20,000 and 40,000 Re for Modified S1223 airfoil

Figure 3 represents the Cl/Cd of the modified S1223 airfoil at 20,000 and 40,000 Re. At Re 20,000, the performance of both the modified airfoils was better than that of the normal airfoil in the AOA range of -4 to 16°. However, the performance of the outward bulge was inferior to the normal airfoil in the same AOA range. The performance was enhanced from the AOA of 8°. An improved performance was observed at higher AOAs for the semicircular outward bulge. The performance of the normal S1210 airfoil was worsened at the AOA of 12° but the modified airfoils showed decreased performance at the AOA of 14°, representing a delayed stall range. The same trend was observed at Re 40,000. The normal airfoil showed better aerodynamic performance than the semicircular outward bulge at the AOA of -4 to 6°. At the AOA of 8°, the performance of the outward bulge airfoil was improved. For Re 40,000, the delayed stall was observed for the modified airfoils. The performance of all the airfoils was similar At the AOA of 14 to 20° but the performance of the modified airfoils was better. The best performance was observed for the semi-circular inward bulge. The S1223 airfoil also showed better results when modified with inward and outward intrusions.

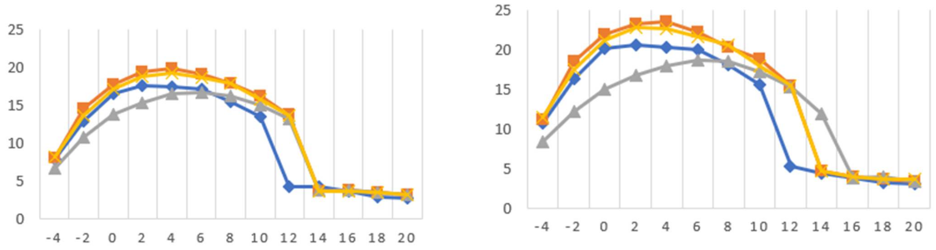

(a) Re 20000 (b) Re 40000

Fig. 3. Cl/Cd of modified S1210 at Re 20,000 and 40,000.

Commented [AZ5]: Please note that all figures in the main text need to be non-editable images.

The performance of the modified S1210 airfoil was better than that of the modified S1223 airfoil. All the geometric modifications for the S1210 airfoil enabled better results than those for the S1223 airfoil with Re 20,000 and 40,000. The outward intrusion of the modified S1210 airfoil enabled the improvement of the performance (Fig. 4).

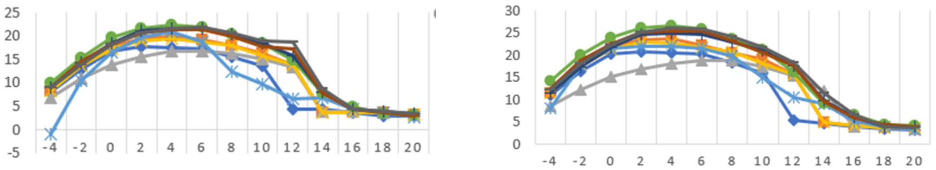

(a) Re 20000 (b) Re 40000

Figure 4. Cl/Cd of modified S1210 an S1223 at Re 20,000 and 40,000.

Commented [AZ6]: Please note that all figures in the main text need to be non-editable images.

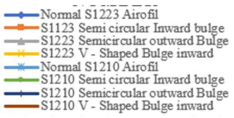

5. Conclusions

We examined the aerodynamic performance of the S1210 and S1223 airfoils under varying conditions and evaluated the effects of geometric modifications, including semi-circular and V-shaped bulges, both inward and outward. The analysis was conducted across a range of Re of 20,000 and 40,000, which are representative of low flow regimes encountered in applications such as small unmanned aerial vehicles, Mars exploration vehicles, and low-speed wind turbines. The analysis results presented that the geometric modifications applied to the airfoils significantly enhanced their aerodynamic performance at Re 20000 and 40000. This improvement was observed across different AOAs, including both positive and negative angles. At higher angles, flow separation and stall occurred. These findings offer a reference to the behavior of modified airfoils in low-Re flows, especially under Martian conditions which are characterized by a thin atmosphere. This numerical analysis results showed that intrusions, or localized geometric modifications on an airfoil's surface improved the performance of the airfoil by influencing the flow behavior and reducing drag, increasing lift, and delaying flow separation. Intrusions create localized accelerations or decelerations in the flow, modifying the pressure distribution on the airfoil. These localized changes induced beneficial turbulence in the boundary layer on the surface for a longer distance along the chord of the airfoil to improve the performance of the airfoil.

Author Contributions: conceptualization, W.C. Wu. and S. Daw; methodology, W.C. Wu. and S. Daw; software, S. Daw; validation, W.C. Wu. and S. Daw; formal analysis, W.C. Wu. and S. Daw; investigation, S. Daw; resources, W.C. Wu. and S. Daw; data curation, S. Daw; writing—original draft preparation, S. Daw; writing—review and editing, W.C. Wu., D. Sharma and S. Daw; visualization, S. Daw; supervision, W.C. Wu.. All authors have read and agreed to the published version of the manuscript.

Commented [AZ7]: Please add these information according to the highlighted comments.

Commented [SD8R7]: Done

Funding: This research did not receive external funding.

Data Availability Statement: The data are not publicly available.

Acknowledgments: This work was support by the Ministry of Science and Technology of the Republic of China under Grand Contract MOST 113-2637-E-150 -006.

Conflicts of Interest: The authors declare no conflict of interest. The funders had no role in the design of the study; in the collection, analyses, or interpretation of data; in the writing of the manuscript, or in the decision to publish the results

References

1. Khater, M. M., & Govindaraj, V. Effectives of Different Shaped Dimples on a NACA Airfoil. *Babylonian Journal of Mechanical Engineering*, **2023**, *8*, 29–37.
2. Wu, W. C., & Kumar, A. Flow past triangular airfoil of variable thickness with low Re in Mars atmosphere. *Numerical Heat Transfer, Part A: Applications* **2024**, 85, 1–21. https://doi.org/10.1080/10407782.2024.2353350
3. Selig, J. Guglielmo, C. Broeren, and J. Giguere. *Summary of low-speed airfoil data*. Virginia, USA: SoarTech Publications. 1995; Volume 3.
4. Nagai, H. Characteristics of low-Re airfoils in a Mars wind tunnel. Proceedings of the 51st AIAA Aerospace Sciences Meeting including the New Horizons Forum and Aerospace Exposition. Grapevine, TX, USA: American Institute of Aeronautics and Astronautics, Jan 7–10, 2013.
5. Munday, P.M., Taira, K., Suwa, T., Numata, D. and Asai, K., 2015. Nonlinear lift on a triangular airfoil in low-Reynolds-number compressible flow. *Journal of Aircraft*, *52*(3), 924–931.